SHORT COMMUNICATIONS

CHARACTERIZATION OF GELATIN FILM WAVEGUIDES

S. SARAT CHANDRA BABU and G. M. NAIK
Department of Electrical Communication Engineering, Indian Institute of Science, Bangalore 560 012, India.

THE possibility of building optical circuits comprising of sources, components and devices in very small dimensions by making use of thin film structures has given birth to the field of integrated optics[1,2]. The successful development of this field depends upon the availability of suitable low loss materials that can be fashioned in the form of thin films. In this paper we present the first experiments on the characterization of gelatin film based two-dimensional light waveguide.

Gelatin is an intergral component of photographic emulsion[3]. It can be obtained in extremely pure form and shows good optical properties such as low absorption and low scattering. Also the refractive index of gelatin can be modulated by appropriate photo-sensitization with ammonium dichromate. Dichromated gelatin (DCG) is considered to be one of the best phase hologram recording medium and in our laboratories we have an ongoing research programme on the characterization of DCG for its use in the development of holographic optical elements (HOEs), with particular emphasis on their application in fibre optic systems. During this research we found that pure gelatin films can be deployed for making thin film optical waveguides.

Fabrication of gelatin based optical waveguide

Good quality gelatin films were obtained by fixing Ilford Zenith photographic plates in Kodak acid fixing salt with hardener baths at 25°C. The fixing time was kept as 10 min to obtain optimum hardening of the gelatin film. The films were then washed in tapwater for 25 min and dried in dust-free environment. The plates were then cut to the required size and mounted on an appropriate base for carrying out the required modal analysis using the prism-coupler technique[4].

Measurements and characterization

The coupling prism is made of EDF glass ($\alpha = 44.92°$, $n_p = 1.694$ at $\lambda = 633$ nm). Linearly polarized light is derived by placing a polarizer in the path of a He–Ne laser beam and depending on the polarizer direction, both transverse electric (TE) and transverse magnetic (TM) modes can be excited separately in the film. The linearly polarized light is directed on to the coupling spot at the prism. The air gap between the film and the prism base has been varied by applying pressure. The whole prism-film assembly is mounted on a turn table so that the mode coupling and the light beam incident angle can be varied at will. At selective incident angles corresponding to the synchronous directions of mode angles of the waveguide, a fine streak of light beam propagates in the film thickness. The highest incident angle of the light beam on the prism face corresponds to the zero order mode of the waveguide. The loss in our waveguide is estimated by using the eye sensitivity method[4] and for the lowest order mode it is observed to be 2.9 dB/cm. For

Table 1 *Optical attenuation in some thin film waveguides at $\lambda = 633$ nm*

Name of the material and substrate	Waveguide loss in dB/cm	References
Gelatin/glass	2.9	Present work
ZnS/glass	5.0	4
ZnO/glass	20.0	4
PCHMA/PMMA	4.0	5
Ta_2O_5/glass	0.9	4
VTMS/glass	0.04	6

Table 2 *β/k values of the waveguide obtained using equation (1)*

	TE modes		TM modes	
Mode No.	Incident angles (degrees)	β/k	Incident angles (degrees)	β/k
0	34.870	1.5300	34.862	1.5299
1	34.831	1.5297	34.829	1.5297
2	34.750	1.5292	34.804	1.5296
3	34.600	1.5282	34.772	1.5294
4	34.455	1.5273	34.651	1.5286
5	34.275	1.5261	34.439	1.5272
6	34.090	1.5249	34.261	1.5260
7	33.840	1.5232	33.055	1.5246
8	33.615	1.5217	33.815	1.5230
9	33.355	1.5199	33.555	1.5213
10	33.030	1.5177	33.265	1.5193

comparison the waveguide loss obtained using other materials at $\lambda = 633$ nm is displayed in table 1 and it can be seen that gelatin is a promising candidate.

To find the mode angles of the waveguide, an output prism coupler is mounted on the film in the path of the light streak. To enable accurate measurement of the mode angles, we made weak input coupling of the light beam and nearly 100% output coupling. By rotating the prism table with respect to the light beam direction various guided modes in the film are excited. The observed incident angles for both TE and TM modes of our film are given in table 2.

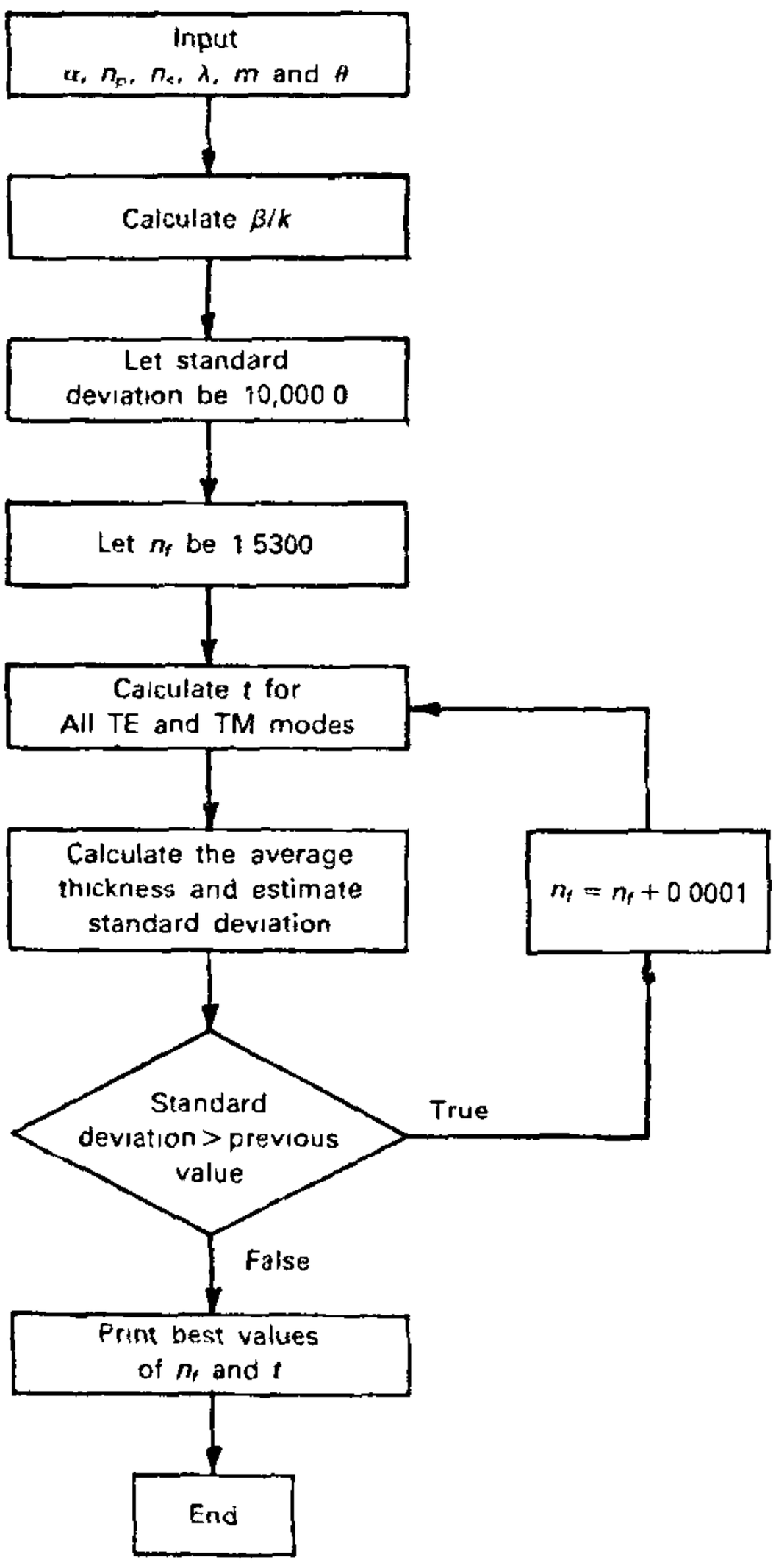

Figure 1. Flow chart for the computer program used.

The important waveguide parameter β/k, which characterizes the guiding property of the film, is calculated using the equation,

$$\beta/k = n_p \sin[\sin^{-1}(\theta_i/n_p) + \alpha] \qquad (1)$$

where β is the propagation constant in the film, k the propagation constant in free space, n_p the refractive index of the prism, θ_i the incident angle on the prism face, and α the prism angle. From the values of β/k measured for different modes, the thickness t and the refractive index of the film, n_f, are calculated by using the following equations.

For TE modes

$$t = \left[\tan^{-1}\left(\frac{(\beta/k)^2 - n_s^2}{n_f^2 - (\beta/k)^2}\right)^{\frac{1}{2}} + \tan^{-1}\left(\frac{(\beta/k)^2 - n_a^2}{n_f^2 - (\beta/k)^2}\right)^{\frac{1}{2}} + m\pi\right] \times \frac{\lambda}{2\pi\sqrt{n_f^2 - (\beta/k)^2}}. \qquad (2)$$

For TM modes

$$t = \left[\tan^{-1}\frac{n_f^2}{n_s^2}\left(\frac{(\beta/k)^2 - n_s^2}{n_f^2 - (\beta/k)^2}\right)^{\frac{1}{2}} + \tan^{-1}\frac{n_f^2}{n_a^2}\left(\frac{(\beta/k)^2 - n_a^2}{n_f^2 - (\beta/k)^2}\right)^{\frac{1}{2}} + m\pi\right] \times \frac{\lambda}{2\pi\sqrt{n_f^2 - (\beta/k)^2}} \qquad (3)$$

where n_a is the refractive index of the air, m the mode number, and n_s the refractive index of the substrate.

A computer program is written to solve the transcendental functions given in (2) and (3) and the flow chart for the same is given in figure 1. The values of t and n_f of the film are calculated using these equations. Thus the estimated thickness of 17.5 μm is found to be in good agreement with the measured (using a Mitutoyo gauge model No. 2109) value of 18 μm. The refractive index is estimated to be 1.5302, which is also in good agreement with the quoted value for gelatin.

It is demonstrated that gelatin-based new thin film optical waveguides can be developed. They are highly transparent, uniform and possess low levels

of scattering and absorption. The measured waveguide loss of 2.9 dB/cm is quite impressive to consider this material as a potential candidate in the fabrication of integrated optical circuits.

5 January 1988

1. Tien, P. K. *et al.*, *Appl. Phys. Lett.*, 1974, **24**, 547.
2. Reinhart, F. K. and Logan, R., A., *Appl. Phys. Lett.*, 1974, **25**, 62.
3. Smith, H. M. (ed.), *Holographic recording materials*, Springer-Verlag, New York, 1977, p. 20.
4. Tien, P. K., *Appl. Opt.*, 1971, **10**, 2395.
5. Ulrich, R. *et al.*, *Appl. Phys. Lett.*, 1972, **20**, 213.
6. Tien, P. K. *et al.*, *Appl. Opt.*, 1972, **11**, 637.

FOSSIL CHAROPHYTA — A SCANNING ELECTRON MICROSCOPIC STUDY AND DEPOSITIONAL ENVIRONMENT

KALYAN CHAKRABORTY
Hydraulic Study Department, Calcutta Port Trust, 20, Garden Reach Road, Calcutta 700 043, India.

SCANNING electron microscopy (SEM) has helped to bring to light the detailed morphology of the fossil Charophyta collected from late Quaternary sediments of Calcutta. In an earlier study, the description was simple because of the limitations of the light microscope. The present investigation provides valuable documentation for identification of fossil Charophyta.

Morphometric measurements on gyrogonites and a simple morphologic description based on light microscopy[1] led to their identification as *Chara fragilis* Desvaux. The present morphologic description is in agreement with the earlier identification.

Daily[2] reported that fossils of *C. fragilis* are related to those of *C. globularis* in morphological features. Tappan[3] also held a similar view. But Soulie-Marsche[4] described *C. globularis* as having concave spiral rims. Interestingly, Bhatia and Mathur[5] found that immature shells of *C. fragilis* show concave spiral rims while the mature ones show convex spiral rims, and in the latter case *C. fragilis* resembles *Grambastichara*. Therefore, it seems that Daily[2] and Tappan[3] observed the immature shells of *C. fragilis*.

The morphometric characteristics of gyrogonites are given in table 1. The gyrogonites are apically somewhat rounded and slightly conical in the basal part. This structure gives rise to their anisopolarity. Both the apex and base, which are circular with pores, are somewhat truncated in the apical peripheral zone in lateral view. Five spiral rims form a hollow and a depression (figures 1 and 2) on the apex which is covered by five plates with relatively smooth, curved outline and a raised partition between plates. The apical plates radiate from a central zone which is much smaller compared to that of the base. The basal plate is however undivided and made up of a simple cell only. On the other hand five basal plates form a truncated pentagonal pyramid (figure 3). The spiral rims appear to be evolved from these basal plates and, interestingly, each of them terminates at the peripheral margin of an apical plate with a pointed end (figure 1). As evident from figures 2 and 4, the surface texture of the rims appears smooth, porous and rugose with gradual increase in magnification. Within the surface there are two sets of elongated fissures and a crack-like feature oblique to the suture line (figures 2 and 4) which is simple; occasionally fine ribs transverse to the suture line are visible. The 'stems' or utricles are like hollow tubes (diameter 300 μm) with longitudinal furrows extending from one end to the other. The longitudinal furrows give rise to plates with a rough, pitted surface not very regular in outline (figure 5). In some cases, the longitudinal furrows are not distinct and a brack-like cell seems to be present in one of the utricles

Table 1 *Morphometric characteristics of gyrogonites*

Sp. No.	Length (μm)	Width (μm)	Thickness of the rims (μm)	No. of rims from lateral view	Iniso-polarity index (ANI)	Remarks
1	600	465	75	10	1.29	Rims convex
2	450	400	60–75	8	1.12	Rims convex
3	570	525	60–75	10	1.00	Rims convex
4	510	405	45–60	10	1.26	Rims convex